Zinc Di(*tert*-butyl)phosphate Complexes as Precursors to Zinc Phosphates. Manipulation of Zincophosphate Structures

Claus G. Lugmair,[†,‡] T. Don Tilley,*[,†,‡] and Arnold L. Rheingold*[,§]

Department of Chemistry, University of California, Berkeley, Berkeley, California 94720-1460; The Chemical Sciences Division, Lawrence Berkeley Laboratory, 1 Cyclotron Road, Berkeley, California 94720; and the Department of Chemistry and Biochemistry, University of Delaware, Newark, Delaware 19716-2522

Received July 17, 1996. Revised Manuscript Received September 17, 1996[⊗]

The reaction of $ZnEt_2$ with $HO(O)P(O^tBu)_2$ gives the insoluble polymer $\{Zn[O_2P(O^tBu)_2]_2\}_n$ (**1**). In the presence of slight amounts of water, this reaction produces good yields of the oxo-centered tetranuclear cluster $Zn_4(\mu_4\text{-}O)[O_2P(O^tBu)_2]_6$ (**2**), which has been characterized by X-ray crystallography. Compound **2** is thermally labile and eliminates isobutene and water over the temperature range 130−220 °C. The ceramic yield at 900 °C corresponds to the theoretical yield for a $Zn_4P_6O_{19}$ material, and the observed products at this temperature are $\alpha\text{-}Zn_2P_2O_7$ and $\beta\text{-}Zn(PO_3)_2$ (by XRD). When heated in ethanol at 85 °C for 30 h, **2** converts to polymer **1** and ZnO. This transformation is facilitated by acids, which allow the conversion to occur at room temperature. Polymer **1**, characterized by X-ray crystallography, adopts a zigzag structure with zinc atoms linked alternately by one and then three bridging phosphate groups. This structure is therefore different from that adopted by the other two organozincophosphate $\{Zn[O_2P(OR)_2]_2\}_n$ polymers that are known, which exist as linear chains with the zinc atoms bridged by two phosphate groups. Polymer **1** undergoes a quantitative pyrolytic conversion to $\beta\text{-}Zn(PO_3)_2$. Diffusion of a toluene solution of **2** into a dichloromethane solution of 1,6-hexanediamine produces a coordination network with the formula $\{Zn[O_2P(O^tBu)_2]_2[H_2N(CH_2)_6NH_2]\}_n$ (**3**), with elimination of ZnO. The network structure of **3** consists of $\{Zn[O_2P(O^tBu)_2]_2[H_2N(CH_2)_6NH_2]\}_n$ polymer strands interconnected via hydrogen bonds between the N−H and P═O groups to form layers stacked along the crystallographic *b* axis. Each polymer chain contains four-coordinate zinc atoms bonded to two monodentate di-*tert*-butylphosphate ligands and linked by 1,6-hexanediamine groups. Slabs of the layered structure are held together by a dense array of hydrogen bonds involving the N−H and P═O functionalities. These layers possess zinc phosphate/1,6-hexanediamine cores and are coated with *tert*-butyl groups such that there are only van der Waals interactions between layers. Thermogravimetric analysis and XRD studies show that **3** undergoes thermolysis to a mixture of crystalline $\alpha\text{-}Zn_2P_2O_7$ and $\beta\text{-}Zn(PO_3)_2$.

Introduction

In recent years, considerable effort has been devoted to the development of molecular routes to advanced materials.[1] Early applications of this approach made use of alkoxide derivatives in "sol−gel" routes to glasses and other ceramic materials.[2] In principle, molecular-level control over the formation of 3-dimensional structures should provide rational syntheses to a wide variety of new materials with tailored properties. One appealing advantage to this strategy is that it can provide atomic-level control over a material's composition and homogeneity, particularly via use of "single-source" molecular precursors.[1,3] We have previously explored the use of metal alkoxy(siloxy) derivatives of the type $M[OSi(O^tBu)_3]_n$ as single-source precursors to metal silicate materials such as $MO_2\cdot nSiO_2$ (M = Ti, Zr, Hf),[4] $3Al_2O_3\cdot 2SiO_2$ (mullite),[5] $Cu\cdot nSiO_2$,[6] $CuO\cdot nSiO_2$,[6] and

[†] University of California, Berkeley.
[‡] Lawrence Berkeley Laboratory.
[§] University of Delaware.
[⊗] Abstract published in *Advance ACS Abstracts,* November 1, 1996.

(1) For example, see: (a) *Ultrastructure Processing of Advanced Materials;* Uhlmann, D. R., Ulrich, D. R., Eds.; Wiley-Interscience: New York, 1992. (b) *Better Ceramics Through Chemistry V;* Materials Research Society Symposia Proceedings, Vol 271; Hampden-Smith, M. J., Klemperer, W. G., Brinker, C. J., Eds.; Materials Research Society: Pittsburgh, 1992. (c) *Inorganic Materials;* Bruce, D. W., O'Hare, D., Eds.; Wiley: New York, 1992. (d) Bowes, C. L.; Ozin, G. A. *Adv. Mater.* **1996**, *8*, 13. (d) Amabilino, D. B.; Stoddart, J. F. *Chem. Rev.* **1995**, *95*, 2725. (e) Stein, A.; Keller, S. W.; Mallouk, T. E. *Science* **1993**, *259*, 1558.

(2) (a) *Sol−Gel Science;* Brinker, C. J.; Scherer, G. W.; Academic Press: Boston, 1990. (b) Hubert-Pfalzgraf, L. G. *New J. Chem.* **1987**, *11*, 663. (c) Mehrotra, R. C. *J. Non-Cryst. Solids* **1988**, *100*, 1. (d) Sanchez, C.; Livage, J.; Henry, M.; Babonneau, F. *J. Non-Cryst. Solids* **1988**, *100*, 165. (e) Chandler, C. D.; Roger, C.; Hampden-Smith, M. J. *Chem. Rev.* **1993**, *93*, 1205. (f) *Sol−Gel Technology for Thin Films, Fibers, Preforms, Electronics, and Specialty Shapes;* Klein, L. C., Ed.; Noyes: Park Ridge, NJ, 1988.

(3) (a) Cowley, A. H.; Jones, R. A. *Angew. Chem., Int. Ed. Engl.* **1989**, *28*, 1208. (b) Williams, A. G.; Interrante, L. V. In *Better Ceramics Through Chemistry;* Materials Research Society Symposia Proceedings, Vol 32, Brinker, C. J., Clark, D. E., Ulrich, D. R., Eds.; North-Holland: New York, 1984; p 152. (c) Apblett, A. W.; Warren, A. C.; Barron, A. R. *Chem. Mater.* **1992**, *4*, 167. (d) Chaput, F.; Lecomte, A.; Dauger, A.; Boilot, J. P. *Chem. Mater.* **1989**, *1*, 199. (e) Hoffman, D. M. *Polyhedron* **1994**, *13*, 1169.

(4) (a) Terry, K. W.; Tilley, T. D. *Chem. Mater.* **1991**, *3*, 1001. (b) Terry, K. W. Ph.D. Thesis, University of California at San Diego, 1993.

(5) Terry, K. W.; Gantzel, P. K.; Tilley, T. D. *Chem. Mater.* **1992**, *4*, 1290.

(6) Terry, K. W.; Lugmair, C. G.; Gantzel, P. K.; Tilley, T. D. *Chem. Mater.* **1996**, *8*, 274.

S0897-4756(96)00382-1 CCC: $14.00

$Zn_2SiO_4 \cdot SiO_2$.[7] These precursor compounds are quite thermally labile and convert to carbon-free materials at very low temperatures (100−200 °C), with clean elimination of water, isobutene, and/or butanol.

In examining the generality of this approach to oxide-based networks, we have recently sought to develop additional multicomponent precursor compounds with high oxygen contents. In this contribution, we describe the synthesis and characterization of precursors based on zinc complexes of the di-*tert*-butylphosphate ligand $^{-}O_2P(O^tBu)_2$. Such precursors were expected to transform via low-energy pathways to zinc phosphate networks based on ZnO_4 and PO_4 tetrahedra. Such networks display a large structural diversity, and recent reports describe zincophosphate and zincophosphonate frameworks which are microporous,[8] layered,[9] or 1-dimensional (polymeric). [10]

Our initial synthetic studies targeted the zinc complex $\{Zn[O_2P(O^tBu)_2]_2\}_n$ (**1**). Previous reports on related zinc complexes include the zinc dialkylphosphinate polymers $[Zn(O_2PR_2)_2]_n$, which consist of a series of zinc atoms bridged alternately by three and one O_2PR_2 ligands.[11] More recently zinc dialkyl phosphate polymers $\{Zn[O_2P(OR)_2]_2\}_n$ (R = Me, Et), which possess two phosphate bridges between pairs of zinc atoms, were reported.[10] No molecular (nonpolymeric) zinc dialkylphosphate complexes have previously been reported, in contrast to the well-known series of zinc O,O′-dialkyldithiophosphate complexes $\{Zn[S_2P(OR)_2]_2\}_n$, which exist as dimers with two bridging $^{-}S_2P(OR)_2$ ligands.[12] This difference may be due to the ability of $-S_2P(OR)_2$ ligands to chelate to a Zn center, whereas $-O_2P(OR)_2$ groups prefer to bridge, thus producing extended chain structures. [12a,13]

Results and Discussion

Synthesis and Characterization of $Zn_4(\mu_4\text{-}O)[O_2P(O^tBu)_2]_6$ (2). Attempts to prepare $Zn[O_2P(O^tBu)_2]_2$ were initially based on the reaction of 2 equiv of $HO(O)P(O^tBu)_2$[14] with $ZnEt_2$. This reaction in pentane solution gave a white insoluble solid which was subsequently shown to be polymeric $\{Zn[O_2P(O^tBu)_2]_2\}_n$ (**1**, 50%), by comparison of its infrared spectrum and powder X-ray diffraction (XRD) pattern to those for an independently prepared sample (vide infra). The pentane filtrate from this reaction contained at least four products, but the species present in highest abundance (ca. 50% of the mixture, ^1H NMR δ 1.58) was fractionally crystallized and identified by X-ray crystallography as the oxo-centered tetranuclear cluster $Zn_4(\mu_4\text{-}O)[O_2P(O^tBu)_2]_6$ (**2**). The remaining soluble products could not be separated by repeated recrystallizations.

Compound **2** presumably forms via a reaction involving adventitious water. In fact, addition of a small amount of water to an ether solution of the soluble product mixture resulted in complete conversion of all species to **2**. Compound **2** is best prepared (61% isolated yield) by combining pentane solutions of $ZnEt_2$ (4 equiv) and $HO(O)P(O^tBu)_2$ (6 equiv) and then adding 1 equiv of water in tetrahydrofuran (eq 1).

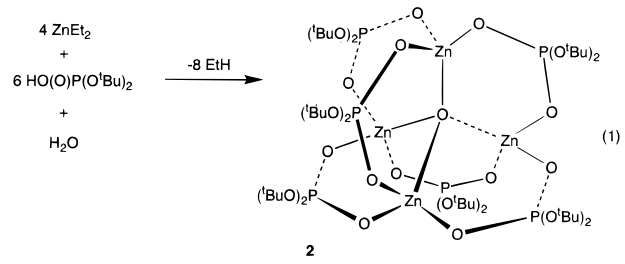

A number of other clusters containing the $Zn_4(\mu_4\text{-}O)$ core are known.[15] For example, the corresponding O,O′-dialkyl dithiophosphate analogue of compound **2**, $Zn_4(\mu_4\text{-}O)[S_2P(O^nBu)_2]_6$, possesses a similar structure.[16] Interestingly, when a toluene solution of this cluster is heated to 80 °C, it reversibly dissociates to $Zn[S_2P(O^iPr)_2]_2$ and ZnO.[17] In contrast, compound **2** remains intact over 24 h when heated to 80 °C in benzene-d_6.

Also, whereas $Zn_4(\mu_4\text{-}O)(\mu\text{-}O_2CMe)_6$ is highly sensitive toward hydrolysis,[18a] compound **2** is air stable in the solid state, and tetrahydrofuran solutions of **2** are only partially hydrolyzed over the course of a week at room temperature when exposed to air. The acetate cluster $Zn_4(\mu_4\text{-}O)(\mu\text{-}O_2CMe)_6$ has been studied as a molecular model for ZnO because of its luminescent properties.[18] The latter cluster possesses an unusual absorption band in the UV−vis spectrum (λ_{max} = 216 nm) which has been

(7) Su, K.; Tilley, T. D.; Sailor, M. J. *J. Am. Chem. Soc.* **1996**, *118*, 3459.

(8) (a) Feng, P.; Bu, X.; Stucky, G. D. *Angew. Chem., Int. Ed. Engl.* **1995**, *34*, 1745. (b) Gier, T. E.; Stucky, G. D. *Nature* **1991**, *349*, 508. (c) Nenoff, T. M.; Harrison, W. T. A.; Gier, T. E.; Stucky, G. D. *J. Am. Chem. Soc.* **1991**, *113*, 378. (d) Harrison, W. T. A.; Gier, T. E.; Moran, K. L.; Nicol, J. M.; Eckert, H.; Stucky, G. D. *Chem. Mater.* **1991**, *3*, 27. (e) Harrison, W. T. A.; Gier, T. E.; Stucky, G. D.; Broach, R. W.; Bedard, R. A. *Chem. Mater.* **1996**, *8*, 145. (f) Harrison, W. T. A.; Broach, R. W.; Bedard, R. A.; Gier, T. E.; Bu, X.; Stucky, G. D. *Chem. Mater.* **1996**, *8*, 691. (g) Song, T.; Hursthouse, M. B.; Chen, J.; Xu, J.; Malik, K. M. A.; Jones, R. H.; Xu, R.; Thomas, J. M. *Adv. Mater.* **1994**, *6*, 679. (h) Whang, D.; Hur, N. H.; Kim, K. *Inorg. Chem.* **1995**, *34*, 3363. (i) Drumel, S.; Janvier, P.; Barboux, P.; Bujoli-Doeuff, M.; Bujoli, B. *Inorg. Chem.* **1995**, *34*, 148. (j) Drumel, S.; Janvier, P.; Deniaud, D.; Bujoli, B. *J. Chem. Soc., Chem. Commun.* **1995**, 1051. (k) Dutta, P. K.; Jakupca, M.; Reddy, K. S. N.; Salvati, L. *Nature* **1995**, *374*, 44.

(9) (a) Ortiz-Avila, C. Y.; Squattrito, P. J.; Shieh, M.; Clearfield, A. *Inorg. Chem.* **1989**, *28*, 2608. (b) Shieh, M.; Martin, K. J.; Squattrito, P. J.; Clearfield, A. *Inorg. Chem.* **1990**, *29*, 958. (c) Poojary, D. M.; Clearfield, A. *J. Am. Chem. Soc.* **1995**, *117*, 11278. (d) Cao, G.; Lee, H.; Lynch, V. M.; Mallouk, T. E. *Inorg. Chem.* **1988**, *27*, 2781. (e) Frink, K. J.; Wang, R.-C.; Colón, J. L.; Clearfield, A. *Inorg. Chem.* **1991**, *30*, 1438. (e) Cao, G.; Mallouk, T. E. *Inorg. Chem.* **1991**, *30*, 1434. (f) Huo, Q.; Margolese, D. I.; Ciesta, U.; Feng, P.; Gier, T. E.; Sieger, P.; Leon, R.; Petroff, P. M.; Schüth, F.; Stucky, G. D. *Nature* **1994**, *368*, 317.

(10) (a) Harrison, W. T. A.; Nenoff, T. M.; Gier, T. E.; Stucky, G. D. *J. Mater. Chem.* **1994**, *4*, 1111. (b) Harrison, W. T. A.; Nenoff, T. M.; Gier, T. E. Stucky, G. D. *Inorg. Chem.* **1992**, *31*, 5395.

(11) (a) Giancotti, V.; Giordano, F.; Randaccio, L.; Ripamonti, A. *J. Chem. Soc.* **1968**, 757 and references therein. (b) Giordano, F.; Randaccio, L.; Ripamonti, A. *Acta Crystallogr., Sect. B* **1969**, *25*, 1057. (c) Giordano, F.; Randaccio, L.; Ripamonti, A. *J. Chem. Soc., Chem. Commun.* **1967**, 19.

(12) (a) Calligaris, M.; Nardin, G.; Ripamonti, A. *J. Chem. Soc. A* **1970**, 714. (b) Lawton, S. L.; Kokotailo, G. T. *Inorg. Chem.* **1969**, *8*, 2410.

(13) Karayannis, N. M.; Mikulski, C. M.; Pytlewski, L. L. *Inorg. Chim. Acta Rev.* **1971**, 69.

(14) Zwierzak, A.; Kluba, M. *Tetrahedron* **1971**, *27*, 3163.

(15) (a) Koyama, H.; Saito, Y. *Bull. Chem. Soc. Jpn.* **1954**, *27*, 112. (b) Cen, W.; Haller, K. J.; Fehlner, T. P. *Inorg. Chem.* **1991**, *30*, 3120. (c) Belforte, A.; Calderazzo, F.; Englert, U.; Strähle, J. *Inorg. Chem.* **1991**, *30*, 3778. (d) Konno, T.; Nagashio, T.; Okamoto, K.; Hidaka, J. *Inorg. Chem.* **1992**, *31*, 1160. (e) Okamoto, K.; Watanabe, Y.; Konno, T.; Hidaka, J. *Bull. Chem. Soc. Jpn.* **1992**, *65*, 3015. (f) Lee, C.-F.; Chin, K.-F.; Peng, S.-M.; Che, C.-M. *J. Chem. Soc., Dalton Trans.* **1993**, 467.

(16) Burn, A. J.; Joyner, R. W.; Meehan, P.; Parker, K. M. A. *J. Chem. Soc., Chem. Commun.* **1986**, 982.

(17) Burn, A. J.; Dewan, S. K.; Gosney, I.; Tan, P. S. G. *J. Chem. Soc., Perkin Trans.* **1990**, 1311.

(18) (a) Kunkely, H.; Vogler, A. *J. Chem. Soc., Chem. Commun.* **1990**, 1204. (b) Bertoncello, R.; Bettinelli, M.; Casarin, M.; Gulino, A.; Tondello, E.; Vittadini, A. *Inorg. Chem.* **1992**, *31*, 1558.

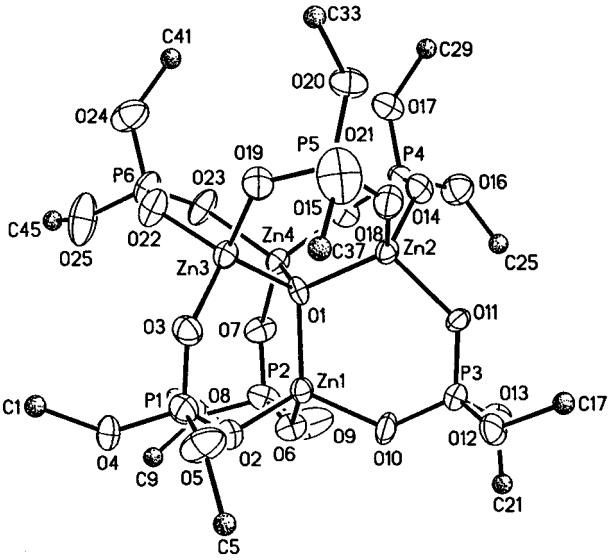

Figure 1. ORTEP view of **2** with atom-labeling scheme for non-hydrogen atoms. Methyl carbon atoms have been removed for clarity.

assigned as an oxygen-to-zinc LMCT transition.[18] In contrast, the phosphate compound **2** does not have an electronic absorption above 190 nm.

An ORTEP drawing of **2** is shown in Figure 1. The cluster may be described as an oxide-centered Zn_4 tetrahedron, bridged on each of the six edges by a $O_2P(O^tBu)_2$ group. The Zn−O(μ_4) bond distances range from 1.968 (13) to 2.010 (12) Å, and the Zn−O(phosphate) distances range from 1.906 (14) to 1.963 (18) Å. These values are similar to those found in $Zn_4O(O_2CMe)_6$ (1.96 and 1.98 Å, respectively).[15a]

To investigate the possible transfer of the $Zn_4(\mu_4\text{-O})$ building block to a zincophosphate network, we examined pyrolytic and hydrolytic conversions of **2** to solid-state materials. We envisioned several approaches for conversions to ordered networks, as outlined below. One approach would involve "preassembly" of **2** into an organized, supramolecular array via interactions (hydrogen or dative bonds) with additional molecules or templates. Such structures may serve as a scaffolding for the directed incorporation of Zn_4O and PO_4 building blocks into novel structures. We therefore investigated the interaction of **2** with a diamine which seemed to have the potential to interconnect the $Zn_4O(PO_4)_6$ molecular units via hydrogen bonding of N−H functionalities to the oxygen atoms in **2**.

Solid-State Thermolysis of $Zn_4(\mu_4\text{-O})[O_2P(O^tBu)_2]_6$ (2). Compound **2** readily loses its hydrocarbon content at low temperature. The thermogravimetric analysis (TGA) curve for **2** under nitrogen reveals two distinct weight losses (Figure 2). The major weight loss (45%) occurs abruptly at 134 °C, and this is followed by a minor reduction in weight of 5% at ca. 224 °C. The differential thermal analysis (DTA) curve (Figure 3) contains two sharp, endothermic peaks corresponding to each weight loss.

To characterize the chemistry of thermolysis a sample of **2** was heated under vacuum, by submersion into a preheated oil bath, and the volatile decomposition products were trapped at −196 °C in an NMR tube. Heating to 155 °C for 5 min produced a colorless, tacky solid, and the volatile products consisted of isobutene and water (7.3:1, by ^{1}H NMR spectroscopy). The

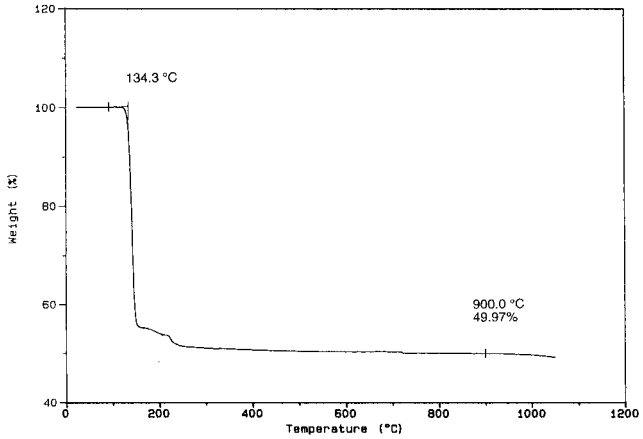

Figure 2. TGA of **2** under N_2. Heating rate 10 °C min^{-1}.

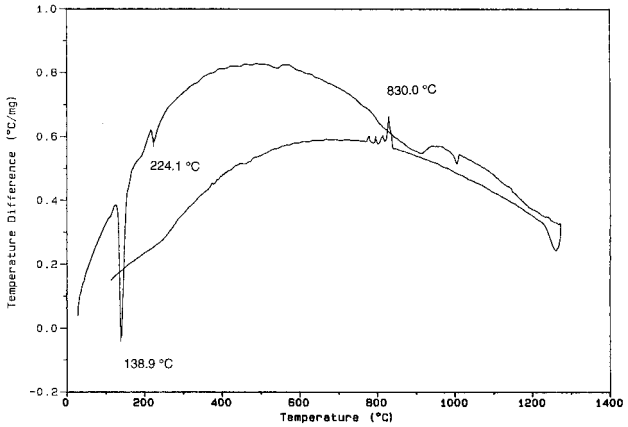

Figure 3. DTA of **2** under N_2. Heating rate 10 °C min^{-1}.

infrared spectrum of the solid product contained a strong absorption at 3400 cm^{-1} for hydroxy groups. Heating a sample of **2** to 300 °C for 1 h resulted in a hard material that contained no hydroxy groups by infrared spectroscopy. The isobutene/water ratio produced at this temperature was 4:1. Thus it appears that the second weight loss observed by TGA corresponds to the condensation of hydroxy groups, with elimination of water.

The ceramic yield of 50.0% observed for compound **2** at 900 °C closely corresponds to the calculated yield for a $Zn_4P_6O_{19}$ material (49.0%). This indicates that no phosphorus is lost as P_2O_5 during the pyrolysis. A bulk sample of **2** which had been heated for 1 h at 300 °C contained only one crystalline component (by XRD), which has been reported as an unindexed phase with the stoichiometry $Zn_2P_2O_7$.[19] Samples heated at 600, 800, and 900 °C (1 h at each temperature) contain significant amounts of α-$Zn_2P_2O_7$ and β-$Zn(PO_3)_2$, as shown by room-temperature XRD patterns.[20] The samples heated to 600 and 800 °C had the appearance of sintered powders, whereas the sample heated to 900 °C had partially melted to form one solid mass. Note that the DTA curve (Figure 3) shows a broad endotherm from 810 to 920 °C corresponding to melting of the $Zn(PO_3)_2$.[20] There is another sharp endotherm at 1005 °C, which is close to the reported melting point of pure $Zn_2P_2O_7$ (1017 °C).[20] An exotherm on the cooling curve

(19) International Center for Diffraction Data "PC-PDF", 1988; Vol. 2, Card 39-711.

(20) Katnack, F. L.; Hummel, F. A. *J. Electrochem. Soc.* **1958**, *105*, 125.

at 830 °C appears to represent the crystallization of a eutectic mixture of $Zn_2P_2O_7$ and $Zn(PO_3)_2$.[20]

Hydrothermal-like Reactions of $Zn_4(\mu_4\text{-}O)[O_2P(O^tBu)_2]_6$ (2). To further investigate the use of compound **2** as a molecular precursor to new materials, we subjected it to hydrothermal-like conditions expected to lead to elimination of isobutene and condensation of zincophosphate networks. One approach involved the combination of 0.04 mmol of **2** and 4 equiv of H_3PO_4 in ca. 1.5 mL of ethanol. Compound **2** is not soluble in ethanol, but the addition of H_3PO_4 converts the precursor to soluble species. When such a mixture was sealed in a 10 mL Pyrex ampule and heated to 60 °C for 16 h, the only observed product (by XRD) was hopeite, $Zn_3(PO_4)_2 \cdot 4H_2O$. Heating the mixture to 85 °C for 56 h produced a white crystalline powder containing $Zn_3(PO_4)_2 \cdot H_2O$ (by XRD). Upon heating the mixture to 130 °C for 56 h, α-$Zn_3(PO_4)_2$ was produced.

When compound **2** was heated in ethanol at 85 °C for 30 h (without H_3PO_4), a white powder displaying a new XRD pattern was produced. This product, which analyzes as $Zn[O_2P(O^tBu)_2]_2$, also forms from reactions of **2** with various acids in organic solvents at room temperature. Thus, it appears that acids react stoichiometrically with 1 equiv of ZnO derived from **2** (eq 2).

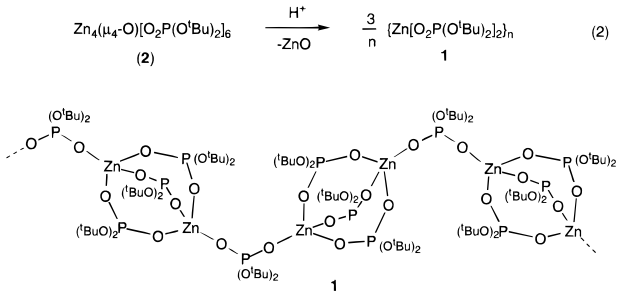

For example, layering a THF solution of **2** above a DMSO solution of terephthalic acid produced colorless single crystals, subsequently identified as the polymer $\{Zn[O_2P(O^tBu)_2]_2\}_n$ (**1**), over 3 days. The same product was obtained as small microcrystals using benzoic acid−DMSO or HCl−DMSO solutions. Smaller crystals of this product also form when the acid solution is layered with a solution of **2** in a solvent less polar than THF. This is presumably due to faster crystallization rates, which result from lower solubility in the less polar medium. Polymer **1** is insoluble in organic solvents, including methanol; however, it is soluble in water.

Polymer **1** was characterized by a single-crystal X-ray structure determination (Figures 4 and 5). The polymer consists of repeat units containing two tetrahedrally coordinated zinc atoms bridged by three di-*tert*-butylphosphate ligands. These units are linked together by one bridging di-*tert*-butylphosphate group to form the polymer chain, which propagates along the *c* direction of the unit cell. The zigzag nature of the polymer backbone requires the *c* direction of the unit cell to span two asymmetric units within one polymer strand. The coordination about the zinc atoms is close to tetrahedral, with O−Zn−O bond angles ranging from 105.3(3) to 116.3(3)° for Zn(1) and from 107.4(3) to 112.8(3)° for Zn(2). The Zn−O bond distances associated with the singly bridging phosphate ligand (1.909(6) and 1.911(6) Å) are slightly shorter than those associated with the triply bridging phosphate groups [1.932(6)−1.948(6) Å for Zn(1); 1.923(7)−1.937(7) Å for Zn(2)]. The Zn−O−P angles associated with the singly bridging phosphate group (148.6(4)−162.9(5)°) are significantly larger than the Zn−O−P angles for the triply bridging phosphates (131.9(4)−138.1(4)°). The independent Zn−Zn distances are 3.79 Å (triply bridged) and 5.62 Å (singly bridged).

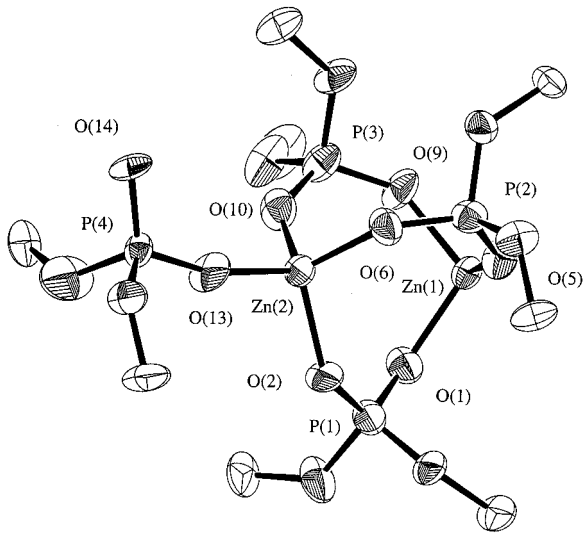

Figure 4. ORTEP view of the asymmetric unit of **1**. Primary carbons and hydrogens have been removed for clarity. Thermal ellipsoids are drawn at 50% probability.

Zinc phosphate **1** belongs to a small class of organozincophosphate materials which exhibit a one-dimensional, polymeric structure. The first examples reported, $\{Zn[O_2P(OMe)_2]_2\}_n$ and $\{Zn[O_2P(OEt)_2]_2\}_n$, consist of linear one-dimensional chains in which adjacent zinc atoms are bridged by two dialkylphosphate groups (structure **A**).[10] This type of polymer backbone structure, which is relatively rare, has also been observed for the phosphinate polymer $[Zn(O_2PHC_6H_5)_2]_n$.[21] Polymer backbones with alternating single and triple bridges, as in **1**, are common for zinc dialkylphosphinate polymers of the type $[Zn(O_2PR_2)_2]_n$.[11] It is not entirely clear why **1** adopts a structure that is different from those of $\{Zn[O_2P(OMe)_2]_2\}_n$ and $\{Zn[O_2P(OEt)_2]_2\}_n$, but the difference may be due to the steric properties of the alkyl groups. The zigzag nature of the polymer backbone may allow for less steric crowding, with more spacing between the bulky ^{t}Bu groups.

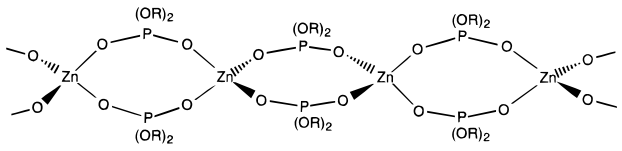

A

Solid-State Thermolysis of $\{Zn[O_2P(O^tBu)_2]_2\}_n$ (1). The TGA trace for **1** (Figure 6) reveals a very abrupt weight loss of 42% at 124 °C, which is followed by a more gradual weight loss of 4%. The initial decomposition gives rise to a sharp endothermic peak in the DTA curve. The ceramic yield at 1000 °C was 46.2%, which is close to the expected yield of 46.16% for $Zn(PO_3)_2$. Thermolysis of a bulk sample of **1** at 800 °C under argon produced β-$Zn(PO_3)_2$ as the only crystal-

(21) Shieh, M.; Martin, K. J.; Squattrito, P. J.; Clearfield, A. *Inorg Chem.* **1990**, *29*, 958.

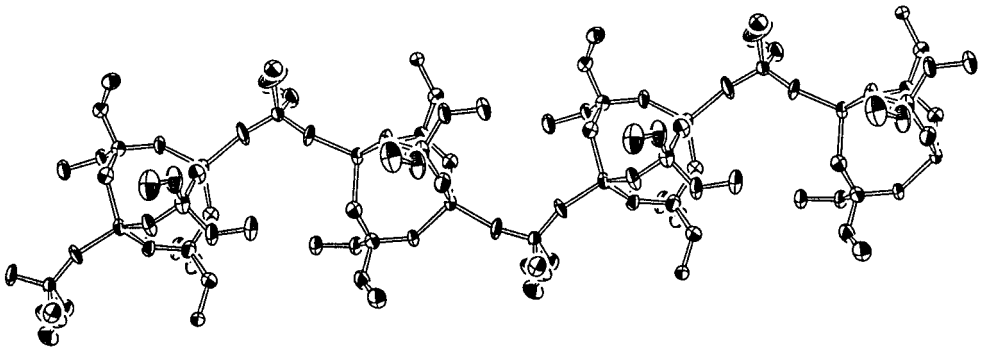

Figure 5. Extended view of the $[Zn_2(O_2P(O^tBu)_2)_4]_n$ polymer. Primary carbons and hydrogens have been removed for clarity. Thermal ellipsoids are drawn at 50% probability.

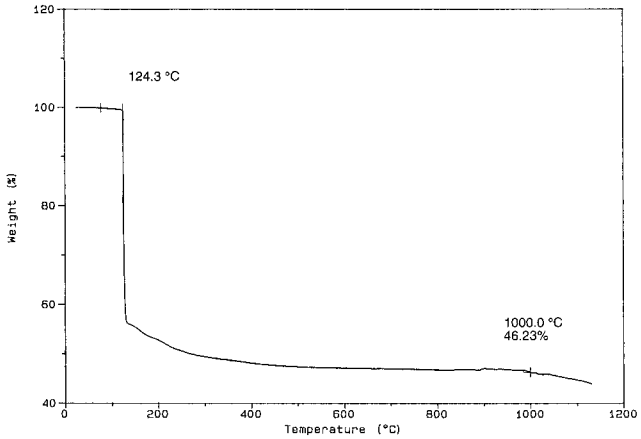

Figure 6. TGA of **1** under N_2. Heating rate 10 °C min^{-1}.

line phase (by XRD), which is the product expected from a precursor with a Zn/P ratio of 0.5.

Formation of the Network Solid $\{Zn[O_2P(O^tBu)_2]_2[H_2N(CH_2)_6NH_2]\}_n$ (3). A crystalline, insoluble diamine adduct (**3**) was isolated by slow (over ca. 4 days) diffusion of a toluene solution of **2** into a dichloromethane solution of 1,6-hexanediamine. This adduct, characterized as a coordination network with the formula $\{Zn[O_2P(O^tBu)_2]_2[H_2N(CH_2)_6NH_2]\}_n$ (vide infra), forms via the formal dissociation of **2** into 3 $Zn[O_2P(O^tBu)_2]_2$ units and 1 equiv of ZnO (eq 3). The assumed ZnO byproduct, which is amorphous by XRD, was readily separated by decantation of a suspension of the finely divided material in toluene from the more crystalline product **3**.

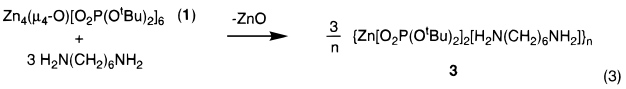

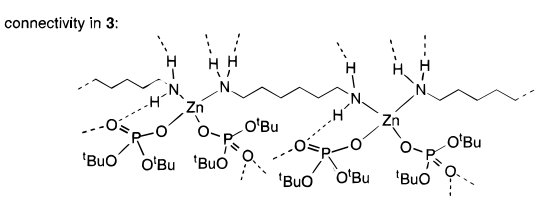

The network structure of **3** consists of $\{Zn[O_2P(O^tBu)_2]_2[H_2N(CH_2)_6NH_2]\}_n$ polymer strands interconnected via hydrogen bonds between the N−H and P═O groups to form layers stacked along the crystallographic *b* axis. The structure therefore resembles that of a "pleated sheet" polypeptide as found, for example, in

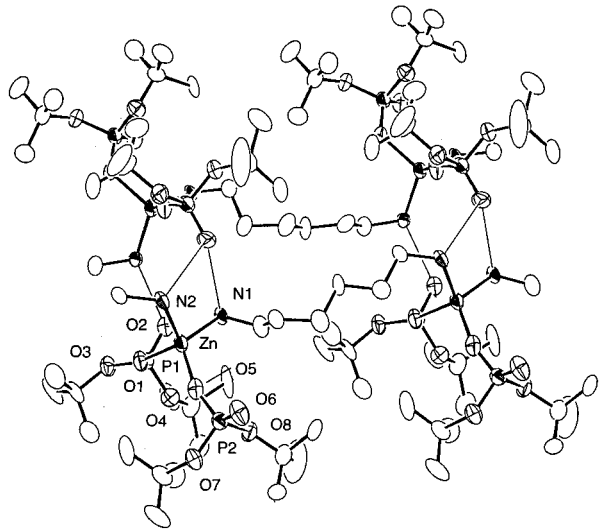

Figure 7. ORTEP view of two polymer chain segments of **3**. Thermal ellipsoids are drawn at 50% probability. Zn, P, and N atoms are represented by shaded octants, the O atoms by unshaded octants, and the C atoms by hollow ellipses. The three short N···O contacts corresponding to interchain hydrogen bonds are indicated by thin solid lines. The intrachain hydrogen bond is omitted for clarity.

β-keratins.[22] Each polymer chain contains four-coordinate zinc atoms bonded to two monodentate di-*t*-butylphosphate ligands and linked by 1,6-hexanediamine groups (Figure 7). Each Zn atom is tetrahedrally coordinated by the oxygen atoms of two monodentate phosphate ligands and the nitrogen atoms of two different 1,6-hexanediamine molecules. Each slab of the layered structure is held together by a dense array of hydrogen bonds involving the N−H and P═O functionalities (Figure 8). The slabs are therefore composed of zinc phosphate/1,6-hexanediamine cores that are coated on either side with terminal *tert*-butyl groups, resulting in only van der Waals interactions between layers. A portion of one layer of **3**, as viewed perpendicular to the polymer chain axis, is shown in the ORTEP drawing of Figure 7. The interchain N···H···O hydrogen bonds, which are represented by thin solid lines, involve three unique N···O contacts of 2.86, 2.83, and 2.94 Å. There is an additional, intrachain hydrogen bond (N(1)···O(2) = 2.96(1) Å) not indicated in Figure 7. One of the phosphate ligands is involved in two external hydrogen bonds and the other in one internal and one external hydrogen bond. The formation of this network seems

(22) Tanford, C. *Physical Chemistry of Macromolecules;* Wiley: New York, 1961, pp 49−54.

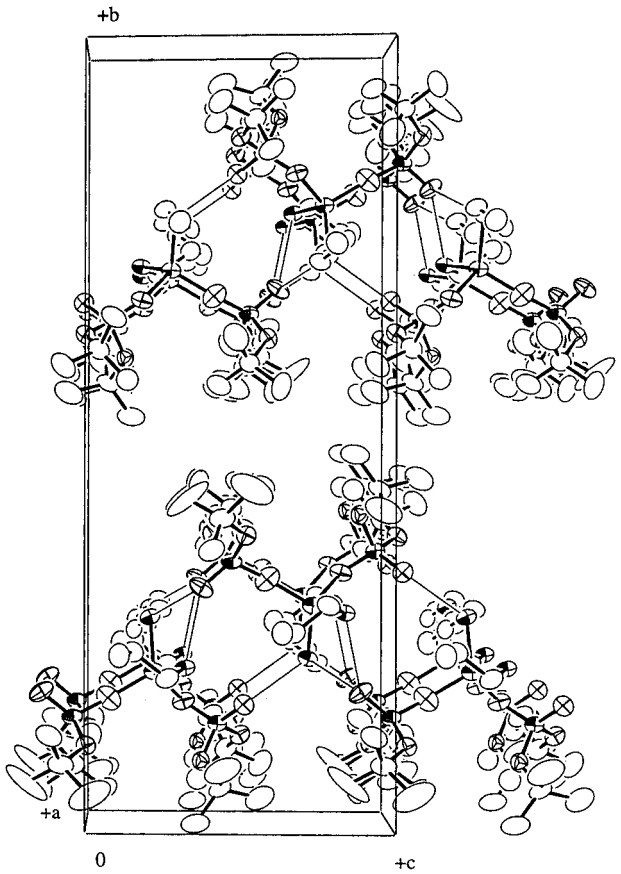

Figure 8. Packing diagram of **3** viewed down the *a* direction. The three short N···O contacts corresponding to interchain hydrogen bonds are indicated by thin solid lines. The intrachain hydrogen bond is omitted for clarity.

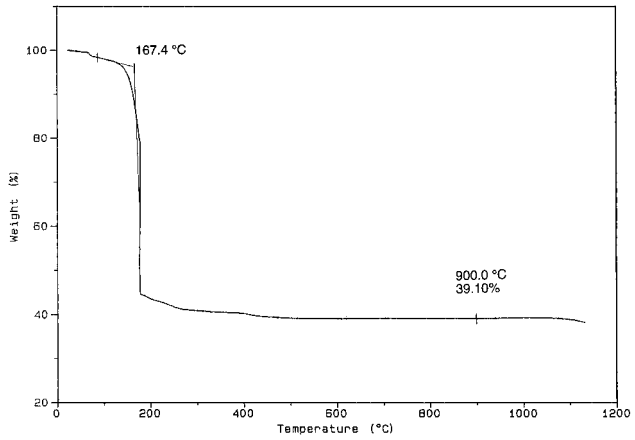

Figure 9. TGA of **3** under N_2. Heating rate 10 °C min^{-1}.

to have a marked effect on the unique Zn−O bond lengths, 1.972(7) and 1.855(9) Å, which differ considerably. The shorter Zn−O bond is associated with a significantly wider Zn−O(5)−P(2) angle (162.7(6)° vs 121.6(5)° for Zn−O(1)−P(1)). Figure 8 provides a partial view of two layers, looking down the polymer chains. This view shows that the polymer strands are packed in a zigzag (up−down) pattern within a layer. Note that for a given polymer chain, the *tert*-butyl groups extend from the same side of the layer.

Solid-State Thermolysis of $\{Zn[O_2P(O^tBu)_2]_2[H_2N(CH_2)_6NH_2]\}_n$ (3). Thermogravimetric analysis of **3** (Figure 9) shows that this compound undergoes a weight loss characterized by an onset temperature of 167 °C. At 900 °C the ceramic yield is 39.1%. Interestingly, **3** is more thermally stable than both **1** and **2**. Thermolysis of a sample of **3** under argon at 600 °C for 1 h yielded a black powder which was not very crystalline, but the XRD pattern for this material matches the unindexed $Zn_2P_2O_7$ phase.[19] The combustion analysis of this material revealed the presence of minimal carbon (1.46%) and no hydrogen or nitrogen (<0.2%). Heating this powder to 800 °C yields a mixture of crystalline α-$Zn_2P_2O_7$ and β-$Zn(PO_3)_2$ (by XRD).

Conclusions

Our synthetic studies on di-*tert*-butylphosphate complexes of zinc have so far yielded polynuclear cluster **2**, polymeric **1**, and 2-dimensional layered **3** structures. This structural diversity is also seen in a variety of structures that have been observed for other zincophosphate networks.[8−10] Thus, combinations of ZnO_4 and PO_4 tetrahedra represent versatile building blocks for the construction of oxide materials. This structural versatility is perhaps due in part to the low bending potential associated with the Zn−O−P linkages, which in this study cover a wide range of bond angles (130−162°).

All of the compounds reported here undergo clean pyrolytic conversions, under mild conditions, to zincophosphate materials. The ceramic yield for compound **2** at 900 °C corresponds to the theoretical yield for $Zn_4P_6O_{19}$, and the observed products at this temperature are α-$Zn_2P_2O_7$ and β-$Zn(PO_3)_2$. Polymer **1** undergoes a quantitative conversion to β-$Zn(PO_3)_2$. Thus, compounds **1**−**3** behave similarly to related alkoxy(siloxy) complexes which convert readily and efficiently to metal silicate materials.[4−7] So far, the observed transformations to phosphate networks have produced only dense, nonporous phases.

The molecular precursor **2** has not been observed to transform to a structure containing the Zn_4O tetrahedral building block, but recent work by Stucky and coworkers indicates that such structures are possible.[8f] Cluster **2** undergoes acid- or base-induced reactions which produce $Zn[O_2P(O^tBu)_2]_2$ units via loss of ZnO. In the future, we hope to make use of this transformation in the construction of new zincophosphate networks. Also, we have observed that under hydrothermal-like conditions using 2-propanol as solvent, combinations of **2** with various diamine "templates" yield new zincophosphate phases which are currently under study. [23]

Experimental Section

General Techniques. All manipulations were performed under a nitrogen atmosphere using standard Schlenk techniques or a Vacuum Atmospheres drybox, unless otherwise noted. Diethyl ether, tetrahydrofuran, and pentane were distilled from sodium benzophenone under nitrogen. Toluene and benzene were distilled from sodium under nitrogen and then degassed. NMR spectra were recorded on a GE QE-300 spectrometer at 300 (^{1}H), 75.5 (^{13}C), or 121.5 (^{31}P) MHz or on a Bruker AMX-400 spectrometer at 400 (^{1}H), 100 (^{13}C), or 161 (^{31}P) MHz. Benzene-d_6 was used as the solvent for all NMR studies. Infrared spectra were collected as Nujol mulls on a Mattson galaxy 3000 spectrometer, using CsI cells. Thermolyses were performed using a Lindberg 1700 °C or a Lindberg 1200 °C three zone tube furnace. Thermal analyses were performed on a DuPont Model 2000 thermal analysis system.

(23) Lugmair, C. G.; Tilley, T. D., work in progress.

Table 1. Atomic Coordinates ($\times 10^4$) and Equivalent Isotropic Displacement Coefficients ($Å^2 \times 10^3$) for $Zn_4(\mu_4\text{-}O)[O_2P(O^tBu)_2]_6$ (2)

atom	*x*	*y*	*z*	U_{eq}[a]	atom	*x*	*y*	*z*	U_{eq}[a]
Zn(1)	1517(1)	4229(1)	1537(1)	37(1)	C(8)	323(11)	3663(18)	247(14)	172(17)
Zn(2)	1980(1)	3477(1)	2591(1)	36(1)	C(9)	1177(11)	6256(18)	1009(15)	102(11)
Zn(3)	1131(1)	4105(1)	2545(1)	40(1)	C(10)	1094(10)	6988(16)	911(13)	137(14)
Zn(4)	1869(1)	5083(1)	2578(1)	38(1)	C(11)	840(19)	5928(30)	1149(26)	408(58)
P(1)	360(2)	4011(3)	1393(3)	54(3)	C(12)	1059(13)	5937(22)	539(17)	238(25)
P(2)	1807(2)	5667(3)	1472(3)	60(3)	C(13)	2421(10)	6429(17)	1379(13)	106(11)
P(3)	2080(2)	3054(3)	1491(3)	43(3)	C(14)	2770(12)	6148(22)	1696(16)	227(23)
P(4)	2641(2)	4407(3)	3261(3)	48(3)	C(15)	2436(9)	6727(15)	841(11)	118(12)
P(5)	1394(2)	2763(3)	3127(3)	62(3)	C(16)	2316(9)	6952(16)	1726(12)	116(12)
P(6)	1195(2)	5469(4)	3129(3)	58(3)	C(17)	2158(7)	1717(12)	1432(10)	59(7)
O(1)	1623(3)	4228(6)	2301(5)	30(5)	C(18)	2105(9)	1317(15)	935(11)	122(12)
O(2)	976(4)	4243(7)	1205(5)	52(6)	C(19)	1964(9)	1450(16)	1824(12)	121(12)
O(3)	716(4)	3889(4)	1965(6)	55(7)	C(20)	2581(7)	1795(14)	1658(10)	89(10)
O(4)	316(5)	4536(10)	1209(7)	90(9)	C(21)	2496(8)	3492(14)	800(11)	82(9)
O(5)	467(5)	3343(9)	1142(7)	87(9)	C(22)	2439(8)	4213(13)	750(10)	94(10)
O(6)	1697(4)	5002(7)	1244(5)	50(6)	C(23)	2245(8)	3141(14)	363(11)	104(11)
O(7)	1901(4)	5742(7)	2041(6)	59(7)	C(24)	2896(10)	3305(18)	784(13)	156(16)
O(8)	1477(10)	6144(10)	1321(11)	233(19)	C(25)	3191(9)	4224(16)	2746(12)	90(9)
O(9)	2152(7)	5882(10)	1255(7)	131(12)	C(26)	3212(10)	3508(15)	2727(13)	134(13)
O(10)	1743(4)	3482(7)	1255(6)	59(7)	C(27)	2915(10)	4416(17)	2271(12)	140(14)
O(11)	2196(4)	3039(6)	2075(5)	41(6)	C(28)	3544(11)	4593(21)	2804(16)	212(21)
O(12)	1968(4)	2361(7)	1252(6)	61(7)	C(29)	2846(9)	4143(15)	4297(12)	83(9)
O(13)	2462(4)	3275(7)	1332(6)	57(7)	C(30)	2885(11)	4544(18)	4742(14)	160(16)
O(14)	2428(4)	3737(7)	3113(5)	48(6)	C(31)	2564(11)	3632(18)	4394(14)	171(17)
O(15)	2386(4)	4981(7)	2988(6)	58(7)	C(32)	3166(11)	3718(18)	4243(14)	171(17)
O(16)	3043(5)	4430(8)	3198(7)	78(8)	C(33)	1361(9)	2505(15)	4126(12)	90(9)
O(17)	2683(5)	4548(7)	3863(6)	63(7)	C(34)	981(9)	2808(15)	4043(12)	122(12)
O(18)	1736(4)	2781(7)	2895(6)	58(7)	C(35)	1353(10)	1760(16)	4174(13)	145(14)
O(19)	1139(4)	3365(8)	3022(6)	62(7)	C(36)	1647(9)	2720(16)	4586(12)	136(14)
O(20)	1570(5)	2657(9)	3731(7)	89(9)	C(37)	873(12)	1967(21)	2483(16)	127(13)
O(21)	1145(6)	2123(9)	2987(10)	106(11)	C(38)	1019(12)	2188(21)	2033(16)	213(21)
O(22)	992(4)	4849(7)	2922(6)	60(7)	C(39)	854(16)	1265(25)	2517(20)	303(34)
O(23)	1577(5)	5544(7)	3017(6)	69(8)	C(40)	516(13)	2195(23)	2520(17)	241(26)
O(24)	1209(5)	5564(10)	3706(7)	90(9)	C(41)	1509(10)	5353(16)	4155(13)	93(10)
O(25)	906(5)	6025(9)	2907(9)	114(12)	C(42)	1913(8)	5660(15)	4209(12)	113(11)
C(1)	-33(11)	4692(18)	1394(14)	107(11)	C(43)	1533(12)	4595(18)	4123(16)	190(19)
C(2)	-228(11)	4099(18)	1517(15)	177(18)	C(44)	1352(11)	5548(19)	4559(14)	176(18)
C(3)	57(9)	5151(16)	1814(12)	122(12)	C(45)	921(17)	6777(27)	2945(22)	189(19)
C(4)	-294(14)	4967(24)	1006(17)	268(28)	C(46)	1274(12)	7006(23)	3073(17)	218(23)
C(5)	430(11)	3155(20)	609(15)	121(12)	C(47)	747(14)	6822(24)	3405(18)	264(28)
C(6)	153(12)	2558(12)	519(15)	211(20)	C(48)	642(16)	6999(29)	2537(20)	357(41)
C(7)	800(11)	2862(19)	556(15)	178(18)					

[a] Equivalent isotropic *U* defined as one-third of the trace of the orthogonalized U_{ij} tensor.

Powder X-ray diffraction was performed on a Siemens D5000 spectrometer. The compounds $H(O)P(O^tBu)_2$[24] and $KO(O)P(O^tBu)_2$[14] were prepared according to literature procedures.

Di-*tert*-butylphosphate. Di-*tert*-butylphosphate was prepared by a modified literature procedure.[14] In a beaker, 5.0 g (0.20 mol) of $KO(O)P(O^tBu)_2$ was dissolved in 25 mL of water. The resulting solution was cooled with an ice bath, and then 3.5 mL (0.042 mol) of a concentrated HCl solution was added over 10 min. The product precipitated as a white solid, and was isolated by filtration and then washed with a small portion of ice cold water. The solid was transferred against a counterflow of nitrogen to a round-bottom flask and then dissolved in 50 mL of pentane. Anhydrous $CaCl_2$ was added to the solution, and the mixture was stirred for 20 min and then filtered. The solution was concentrated under reduced pressure and cooled to −35 °C to afford colorless crystals in 80% yield.

Reaction of $ZnEt_2$ with 2 equiv of $HO(O)P(O^tBu)_2$. A 1.0 M solution of $ZnEt_2$ in hexane (0.85 mL, 0.85 mmol) was added to 20 mL of pentane, and the resulting solution was cooled to −40 °C. The dropwise addition of $HO(O)P(O^tBu)_2$ (0.36 g, 1.7 mmol) in pentane (25 mL) over 15 min yielded a clear solution. The reaction mixture was allowed to warm slowly to room temperature, and this resulted in the formation of a white precipitate. The reaction mixture was stirred for an additional 12 h. The reaction mixture was filtered to give a colorless solution which was evaporated under vacuum to afford a white solid. A ^1H NMR spectrum of this solid revealed the presence of a mixture of products containing **2** as the primary component. The precipitate formed in the reaction was identified as the polymer **1** (50% yield) by XRD and IR spectroscopy.

$Zn_4(\mu_4\text{-}O)[O_2P(O^tBu)_2]_6$ (2). A 1.0 M solution of $ZnEt_2$ in hexane (3.0 mL, 3.0 mmol) was added to 30 mL of pentane, and the resulting solution was cooled to −40 °C. A pentane solution (30 mL) of $HO(O)P(O^tBu)_2$ (0.946 g, 4.5 mmol) was then added dropwise. The resulting reaction mixture was allowed to warm slowly to room temperature and was then stirred for an additional 30 min. This solution was cooled to −40 °C, and a solution of H_2O (0.0135 mL, 0.75 mmol) in 3 mL of THF was added slowly. The reaction mixture was slowly warmed to room temperature and allowed to stir for an additional 12 h. The solvent was removed under reduced pressure, and the resulting white solid was dissolved in pentane (25 mL). The pentane solution was filtered, concentrated, and cooled to −78 °C to afford **2** as a white powder in 61% yield. Anal. Calcd for $Zn_4P_6O_{25}C_{48}H_{108}$: C, 37.61; H, 7.10. Found: C, 37.71; H, 6.95. ^1H NMR (400 MHz) δ 1.58 (s). $^{13}C\{^1H\}$ NMR (100 MHz) δ 30.45 (d, $^3J_{CP} = 5$ Hz), 79.65 (d, $^2J_{CP} = 7$ Hz). $^{31}P\{H\}$ NMR (161.9 MHz) δ −5.27 (s). IR (Nujol, CsI, cm^{-1}) 1392 (w), 1369 (m), 1248 (m), 1082 (s), 1039 (w), 1001 (m), 916 (w), 833 (w), 723 (w), 453 (w).

$\{Zn[O_2P(O^tBu)_2]_2\}_n$ (1). Although other acids can be used to synthesize **1**, this procedure produced the largest crystals. A 15 mL THF solution of **2** (0.050 g, 0.033 mmol) was layered above a 15 mL DMSO solution of terephthalic acid (0.011 g,

(24) Goldwhite, H.; Saunders, B. C. *J. Chem. Soc.* **1957**, 2409.

Table 2. Selected Interatomic Distances (Å) and Angles (deg) for $Zn_4(\mu_4\text{-}O)[O_2P(O^tBu)_2]_6$ (2)

(a) Bond Distances

Zn(1)−O(1)	1.97(1)	Zn(1)−O(2)	1.91(1)
Zn(1)−O(6)	1.92(1)	Zn(1)−O(10)	1.94(2)
Zn(2)−O(1)	2.01(1)	Zn(2)−O(11)	1.93(2)
Zn(2)−O(14)	1.91(1)	Zn(2)−O(18)	1.92(2)
Zn(3)−O(1)	2.01(1)	Zn(3)−O(3)	1.91(1)
Zn(3)−O(19)	1.95(2)	Zn(3)−O(22)	1.93(2)
Zn(4)−O(1)	2.00(1)	Zn(4)−O(7)	1.95(2)
Zn(4)−O(15)	1.91(1)	Zn(4)−O(23)	1.96(2)
P(1)−O(2)	1.50(2)	P(1)−O(3)	1.49(2)
P(1)−O(4)	1.53(2)	P(1)−O(5)	1.56(2)
P(2)−O(6)	1.49(2)	P(2)−O(7)	1.47(2)
P(2)−O(8)	1.50(3)	P(2)−O(9)	1.53(3)
P(3)−O(10)	1.49(2)	P(3)−O(11)	1.50(2)
P(3)−O(12)	1.55(2)	P(3)−O(13)	1.58(2)
P(4)−O(14)	1.52(2)	P(4)−O(15)	1.50(2)
P(4)−O(16)	1.57(2)	P(4)−O(17)	1.58(2)
P(5)−O(18)	1.48(2)	P(5)−O(19)	1.50(2)
P(5)−O(20)	1.59(2)	P(5)−O(21)	1.56(2)
P(6)−O(22)	1.48(2)	P(6)−O(23)	1.46(2)
P(6)−O(24)	1.53(2)	P(6)−O(25)	1.54(2)

(b) Bond Angles

O(1)−Zn(1)−O(2)	113.6(6)	O(1)−Zn(1)−O(6)	114.5(5)
O(2)−Zn(1)−O(6)	101.2(6)	O(1)−Zn(1)−O(10)	113.5(6)
O(2)−Zn(1)−O(10)	107.1(6)	O(6)−Zn(1)−O(10)	105.9(7)
O(1)−Zn(2)−O(11)	113.3(5)	O(1)−Zn(2)−O(14)	114.1(5)
O(11)−Zn(2)−O(14)	103.8(6)	O(1)−Zn(2)−O(18)	114.1(6)
O(11)−Zn(2)−O(18)	104.5(6)	O(14)−Zn(2)−O(18)	106.0(6)
O(1)−Zn(3)−O(3)	109.4(6)	O(1)−Zn(3)−O(19)	114.8(6)
O(3)−Zn(3)−O(19)	103.6(6)	O(1)−Zn(3)−O(22)	114.5(6)
O(3)−Zn(3)−O(22)	110.5(6)	O(19)−Zn(3)−O(22)	103.3(7)
O(1)−Zn(4)−O(7)	113.9(6)	O(1)−Zn(4)−O(15)	113.1(5)
O(7)−Zn(4)−O(15)	106.0(7)	O(1)−Zn(4)−O(23)	112.5(6)
O(7)−Zn(4)−O(23)	104.2(7)	O(15)−Zn(4)−O(23)	106.5(7)
O(2)−P(1)−O(3)	113.5(8)	O(2)−P(1)−O(4)	105.4(10)
O(3)−P(1)−O(4)	113.4(10)	O(2)−P(1)−O(5)	112.4(10)
O(3)−P(1)−O(5)	104.8(9)	O(4)−P(1)−O(5)	107.4(10)
O(6)−P(2)−O(7)	117.4(9)	O(6)−P(2)−O(8)	111.3(12)
O(7)−P(2)−O(8)	101.4(14)	O(6)−P(2)−O(9)	105.1(11)
O(7)−P(2)−O(9)	110.7(10)	O(8)−P(2)−O(9)	111.1(15)
O(10)−P(3)−O(11)	116.3(9)	O(10)−P(3)−O(12)	104.7(8)
O(11)−P(3)−O(12)	112.5(8)	O(10)−P(3)−O(13)	112.1(9)
O(11)−P(3)−O(13)	103.6(8)	O(12)−P(3)−O(13)	107.5(9)
O(14)−P(4)−O(15)	114.5(8)	O(14)−P(4)−O(16)	111.9(9)
O(15)−P(4)−O(16)	110.7(10)	O(14)−P(4)−O(17)	112.0(9)
O(15)−P(4)−O(17)	106.4(9)	O(16)−P(4)−O(17)	100.3(9)
O(18)−P(5)−O(19)	114.8(10)	O(18)−P(5)−O(20)	104.6(10)
O(19)−P(5)−O(20)	112.1(10)	O(18)−P(5)−O(21)	113.0(12)
O(19)−P(5)−O(21)	110.3(10)	O(20)−P(5)−O(21)	101.1(12)
O(22)−P(6)−O(23)	113.9(10)	O(22)−P(6)−O(24)	112.0(11)
O(23)−P(6)−O(24)	112.0(10)	O(22)−P(6)−O(25)	104.8(10)
O(23)−P(6)−O(25)	114.2(11)	O(24)−P(6)−O(25)	98.7(12)
Zn(1)−O(1)−Zn(2)	110.1(6)	Zn(1)−O(1)−Zn(3)	111.1(5)
Zn(2)−O(1)−Zn(3)	107.4(6)	Zn(1)−O(1)−Zn(4)	109.6(6)
Zn(2)−O(1)−Zn(4)	109.5(5)	Zn(3)−O(1)−Zn(4)	109.0(6)
Zn(1)−O(2)−P(1)	130.7(9)	Zn(3)−O(3)−P(1)	135.4(10)
Zn(1)−O(6)−P(2)	130.8(10)	Zn(4)−O(7)−P(2)	131.2(9)
Zn(1)−O(10)−P(3)	130.8(9)	Zn(2)−O(11)−P(3)	131.3(8)
Zn(2)−O(14)−P(4)	131.9(8)	Zn(4)−O(15)−P(4)	134.1(9)
Zn(2)−O(18)−P(5)	132.9(9)	Zn(3)−O(19)−P(5)	131.1(11)
Zn(3)−O(22)−P(6)	133.4(10)	Zn(4)−O(23)−P(6)	135.5(10)

0.065 mmol). Colorless block crystals of the product formed over 3 days on the walls of the flask. The solvent was removed via cannula, and the crystals were dried under reduced pressure affording **1** in 38% yield. Crystals of **1** are insoluble in organic solvents including THF, DMSO, and ethanol. Compound **1** does dissolve in water. Anal. Calcd for $Zn_2P_4O_{16}C_{32}H_{72}$: C, 39.72; H, 7.50. Found: C, 39.40; H, 7.66. IR (KBr pellet, cm^{-1}) 2979 (m), 2933 (w), 1595 (w), 1477 (w), 1394 (w), 1369 (m), 1252 (s), 1184 (s), 1111 (m, sh), 1078 (s), 1039 (m), 997 (s), 918 (w), 833 (w), 725 (w, sh), 710 (w), 596 (w), 552 (w).

$\{Zn[O_2P(O^tBu)_2]_2[H_2N(CH_2)_6NH_2]\}_n$ (3). A toluene solution (7 mL) of **1** (0.05 g, 0.03 mmol) was layered onto a dichloromethane solution (7 mL) of 1,6-hexanediamine (0.011 g, 0.098 mmol). Crystals of **3** grew on the walls of the flask over 4 days. The solvent was removed via cannula, and the crystals were dried under reduced pressure affording **3** in 51% yield. Compound **3** was found to be insoluble in toluene, THF, ethanol, and water. Anal. Calcd for $ZnP_2N_2O_8C_{22}H_{52}$: C, 44.04; H, 8.74; N, 4.67. Found: C, 43.72; H, 8.69; N, 4.64. IR (Nujol, CsI, cm^{-1}) 3180 (m, br), 3103 (m, br), 1626 (w), 1365 (m), 1252 (w, sh), 1240 (w, sh), 1211 (m), 1190 (m), 1103 (m), 1060 (m), 1035 (w), 1003 (w, sh), 982 (s), 916 (w), 829 (w), 719 (w), 604 (w), 553 (w), 491 (w), 470 (w).

Table 3. Atomic Coordinates and Equivalent Isotropic Displacement Coefficients for $\{Zn[O_2P(O^tBu)_2]_2\}_n$ (1)

atom	*x*	*y*	*z*	B_{eq}[a]
Zn(1)	0.74596(6)	−0.31495(9)	0.84136(6)	2.30(3)
Zn(2)	0.76582(6)	−0.17078(9)	0.65894(6)	2.58(3)
P(1)	0.7982(2)	−0.0934(2)	0.8267(1)	3.20(7)
P(2)	0.8381(1)	−0.3740(2)	0.7026(1)	2.90(7)
P(3)	0.6352(1)	−0.2887(2)	0.7107(2)	3.44(7)
P(4)	0.7554(1)	−0.0482(2)	0.4946(1)	2.27(6)
O(1)	0.7524(3)	−0.1724(5)	0.8586(3)	3.5(2)
O(2)	0.8032(4)	−0.0929(5)	0.7418(3)	3.4(2)
O(3)	0.7750(4)	0.0125(5)	0.8554(4)	4.4(2)
O(4)	0.8708(3)	−0.1006(5)	0.8592(3)	2.9(2)
O(5)	0.8229(3)	−0.3595(5)	0.7850(3)	3.1(2)
O(6)	0.8185(4)	−0.2903(5)	0.6508(3)	3.6(2)
O(7)	0.8033(3)	−0.4688(5)	0.6673(3)	2.9(2)
O(8)	0.9146(3)	−0.3972(5)	0.6933(3)	3.2(2)
O(9)	0.6647(3)	−0.3335(5)	0.7819(3)	3.5(2)
O(10)	0.6735(4)	−0.2071(5)	0.6737(4)	4.1(2)
O(11)	0.5655(4)	−0.2393(6)	0.7245(4)	4.8(2)
O(12)	0.6240(3)	−0.3830(5)	0.6569(3)	3.4(2)
O(13)	0.7692(4)	−0.0903(6)	0.5698(3)	4.2(2)
O(14)	0.7315(3)	−0.1196(5)	0.4355(3)	3.0(2)
O(15)	0.8192(3)	0.0042(5)	0.4639(3)	3.3(2)
O(16)	0.7068(4)	0.0430(6)	0.4984(5)	6.1(3)
C(1)	0.7229(6)	0.0748(9)	0.8298(6)	4.1(3)
C(2)	0.7102(9)	0.148(1)	0.8908(8)	7.7(5)
C(3)	0.733(1)	0.117(1)	0.7550(8)	8.5(6)
C(4)	0.6608(8)	0.007(1)	0.8184(9)	8.9(5)
C(5)	0.8953(6)	−0.1165(8)	0.9398(5)	3.7(3)
C(6)	0.8706(6)	−0.2165(8)	0.9679(5)	3.8(3)
C(7)	0.9699(7)	−0.1195(9)	0.9336(6)	4.7(3)
C(8)	0.8719(6)	−0.0299(9)	0.9865(6)	4.4(3)
C(9)	0.7960(6)	−0.5712(7)	0.6987(5)	3.1(3)
C(10)	0.7490(7)	−0.5696(9)	0.7621(7)	5.9(4)
C(11)	0.7671(8)	−0.6290(9)	0.6333(7)	5.9(4)
C(12)	0.8632(8)	−0.6103(10)	0.7215(8)	7.0(5)
C(13)	0.9716(6)	−0.3404(9)	0.7224(6)	3.7(3)
C(14)	0.9587(7)	−0.226(1)	0.7163(8)	6.4(4)
C(15)	0.9826(7)	−0.368(1)	0.8025(7)	6.9(5)
C(16)	1.0283(7)	−0.365(1)	0.6752(8)	7.1(5)
C(17)	0.5163(7)	−0.257(1)	0.7774(7)	5.6(4)
C(18)	0.5370(7)	−0.229(1)	0.8543(7)	8.1(5)
C(19)	0.4535(6)	−0.213(1)	0.7523(9)	7.3(5)
C(20)	0.5077(8)	−0.377(2)	0.7746(8)	8.2(6)
C(21)	0.6051(6)	−0.3809(9)	0.5760(5)	3.8(3)
C(22)	0.5465(6)	−0.315(1)	0.5609(6)	5.2(4)
C(23)	0.5866(7)	−0.490(1)	0.5606(6)	5.7(4)
C(24)	0.6661(7)	−0.353(1)	0.5320(7)	5.9(4)
C(25)	0.8698(6)	0.0625(9)	0.5046(6)	4.1(3)
C(26)	0.9165(6)	−0.010(1)	0.5451(7)	6.1(4)
C(27)	0.9061(8)	0.117(1)	0.4440(8)	7.8(5)
C(28)	0.8397(7)	0.132(1)	0.5604(8)	6.6(4)
C(29)	0.6351(5)	0.0493(9)	0.4973(6)	3.3(3)
C(30)	0.6208(8)	0.146(1)	0.535(1)	9.9(6)
C(31)	0.6149(10)	0.052(2)	0.4177(9)	10.5(7)
C(32)	0.6055(9)	−0.031(1)	0.539(1)	11.7(7)

[a] $B_{eq} = {}^8/_3\pi^2(U_{11}(aa^*)^2 + U_{22}(bb^*)^2 + U_{33}(cc^*)^2 + 2U_{12}(aa^*bb^*) \times \cos\gamma + 2U_{13}(aa^*cc^*)\cos\beta + 2U_{23}(bb^*cc^*)\cos\alpha)$.

X-ray Crystallography. The crystallographic analysis of **2** was carried out at the University of Delaware, and the structures of **1** and **3** were determined at the University of California. Crystallographic data are collected in Table 7.

2: Crystals were grown from a concentrated hexamethyldisiloxane solution at −35 °C. All specimens examined diffracted weakly and appeared somewhat opalescent suggesting the partial loss of solvent, hexamethyldisiloxane. Photo-

Table 4. Selected Interatomic Distances (Å) and Angles (deg) for $\{Zn[O_2P(O^tBu)_2]_2\}_n$ (1)

(a) Bond Distances

Zn(1)−O(1)	1.935(7)	P(2)−O(5)	1.507(6)
Zn(1)−O(5)	1.948(6)	P(2)−O(6)	1.494(7)
Zn(1)−O(9)	1.932(6)	P(2)−O(7)	1.570(7)
Zn(1)−O(14)	1.909(6)	P(2)−O(8)	1.576(7)
Zn(2)−O(2)	1.933(6)	P(3)−O(9)	1.503(7)
Zn(2)−O(6)	1.923(7)	P(3)−O(10)	1.494(7)
Zn(2)−O(10)	1.937(7)	P(3)−O(11)	1.569(8)
Zn(2)−O(13)	1.911(6)	P(3)−O(12)	1.593(7)
P(1)−O(1)	1.518(7)	P(4)−O(13)	1.464(6)
P(1)−O(2)	1.507(6)	P(4)−O(14)	1.487(6)
P(1)−O(3)	1.578(7)	P(4)−O(15)	1.565(7)
P(1)−O(4)	1.555(7)	P(4)−O(16)	1.565(8)

(b) Bond Angles

O(1)−Zn(1)−O(5)	109.3(3)	O(6)−P(2)−O(8)	109.1(4)
O(1)−Zn(1)−O(9)	105.3(3)	O(7)−P(2)−O(8)	102.9(4)
O(1)−Zn(1)−O(14)	109.0(3)	O(9)−P(3)−O(10)	117.6(4)
O(5)−Zn(1)−O(9)	110.5(3)	O(9)−P(3)−O(11)	111.9(4)
O(5)−Zn(1)−O(14)	116.3(3)	O(9)−P(3)−O(12)	103.3(4)
O(9)−Zn(1)−O(14)	105.7(3)	O(10)−P(3)−O(11)	103.2(5)
O(2)−Zn(2)−O(6)	107.5(3)	O(10)−P(3)−O(12)	112.6(4)
O(2)−Zn(2)−O(10)	112.8(3)	O(11)−P(3)−O(12)	108.2(4)
O(2)−Zn(2)−O(13)	107.4(3)	O(13)−P(4)−O(14)	116.1(4)
O(6)−Zn(2)−O(10)	109.2(3)	O(13)−P(4)−O(15)	110.4(4)
O(6)−Zn(2)−O(13)	112.2(3)	O(13)−P(4)−O(16)	111.5(5)
O(10)−Zn(2)−O(13)	107.8(3)	O(14)−P(4)−O(15)	107.3(4)
O(1)−P(1)−O(2)	115.3(4)	O(14)−P(4)−O(16)	109.9(4)
O(1)−P(1)−O(3)	108.8(4)	O(15)−P(4)−O(16)	100.3(5)
O(1)−P(1)−O(4)	112.8(4)	Zn(1)−O(1)−P(1)	131.9(4)
O(2)−P(1)−O(3)	110.0(4)	Zn(2)−O(2)−P(1)	135.9(4)
O(2)−P(1)−O(4)	106.5(4)	Zn(1)−O(5)−P(2)	135.6(4)
O(3)−P(1)−O(4)	102.6(4)	Zn(2)−O(6)−P(2)	135.7(4)
O(5)−P(2)−O(6)	116.1(4)	Zn(1)−O(9)−P(3)	135.5(4)
O(5)−P(2)−O(7)	112.9(4)	Zn(2)−O(10)−P(3)	138.1(4)
O(5)−P(2)−O(8)	110.2(4)	Zn(2)−O(13)−P(4)	162.9(5)
O(6)−P(2)−O(7)	104.8(4)	Zn(1)−O(14)−P(4)	148.6(4)

graphic evidence and systematic absences in the diffraction data indicated either of the monoclinic space groups *Cc* or *C*2/*c*. Processing was confined to the centrosymmetric alternative which refined nicely and produced chemically reasonable bond parameters. No correction for absorption was required (max/min trans ratio = 1.09). The Zn atoms were located by direct methods. A chemically unrecognizable group of residual electron density peaks (max = 1.3 e Å^{-3}), well removed from the main molecule, undoubtedly represents solvent residuum. However, these contributions were not included in the refinement. Due to data limitations, anisotropic refinement was confined to Zn, P, and O atoms only. Hydrogen atom contributions were idealized. All computations used SHELXTL 4.2 software (G. Sheldrick, Siemens XRD, Madison, WI).

1: A colorless block of dimensions 0.12 × 0.11 × 0.10 mm was mounted on a glass fiber using Paratone N hydrocarbon oil. Data were collected using a Siemens SMART diffractometer with a CCD area detector. A preliminary orientation matrix and unit cell parameters were determined by collecting 60 10-s frames, followed by spot integration and least-squares refinement. A hemisphere of data was collected using ω scans of 0.3° and a collection time of 30 s per frame. Frame data were integrated (XY spot spread = 1.60°; *Z* spot spread = 0.60°) using SAINT. The data were corrected for Lorentz and polarization effects. An absorption correction was not necessary. The 19 132 integrated reflections were averaged in point group 2/*m* to give 7205 unique reflections (R_{int} = 0.086). Of these, 4035 reflections were considered observed ($I > 3.00\sigma(I)$). No decay correction was necessary. Inspection of the systematic absences uniquely defined the space group as $P2_1/c$. The structure was solved using direct methods (SAPI91), expanded using Fourier techniques (DIRDIF92), and refined by full-matrix least-squares methods using teXsan software. The non-hydrogen atoms were refined anisotropically. The hydrogen atoms were included at calculated positions but not refined. The number of variable parameters was 487 giving a data/parameter ratio of 8.32. The maximum and minimum peaks on the final difference Fourier map corresponded to 1.15 and −0.59 e$^-$/Å^3: R = 0.075, R_w = 0.078, GOF = 2.59.

Table 5. Atomic Coordinates and Equivalent Isotropic Displacement Coefficients for $\{Zn[O_2P(O^tBu)_2]_2[H_2N(CH_2)_6NH_2]\}_n$ (3)

atom	*x*	*y*	*z*	B_{eq}[a]
Zn	−0.2676(1)	0.20930(4)	0.2232(1)	2.80(6)
P(1)	−0.1803(3)	0.1434(1)	0.4248(3)	2.8(2)
P(2)	−0.3474(3)	0.1546(1)	−0.0334(3)	3.0(2)
O(1)	−0.1408(7)	0.1703(2)	0.3177(7)	3.4(4)
O(2)	−0.2666(8)	0.1685(2)	0.5079(7)	3.6(4)
O(3)	−0.0544(8)	0.1263(2)	0.4994(7)	3.4(4)
O(4)	−0.2518(7)	0.0985(2)	0.3720(6)	3.3(4)
O(5)	−0.2880(8)	0.1767(3)	0.0805(8)	4.8(5)
O(6)	−0.3957(8)	0.1862(3)	−0.1294(8)	4.3(4)
O(7)	−0.2418(7)	0.1223(3)	−0.0932(7)	3.6(4)
O(8)	−0.4588(8)	0.1220(2)	0.0105(7)	3.4(4)
N(1)	−0.4316(9)	0.2162(3)	0.3197(8)	2.6(4)
N(2)	−0.2030(9)	0.2754(3)	0.2109(8)	2.8(4)
C(1)	0.071(1)	0.1067(4)	0.456(1)	3.8(7)
C(2)	0.149(1)	0.1464(4)	0.407(1)	5.0(7)
C(3)	0.136(1)	0.0864(5)	0.568(1)	5.3(8)
C(4)	0.043(1)	0.0691(4)	0.364(1)	4.5(7)
C(5)	−0.338(1)	0.0665(4)	0.431(1)	3.9(7)
C(6)	−0.473(1)	0.0919(5)	0.437(2)	7(1)
C(7)	−0.284(1)	0.0540(5)	0.5568(1)	5.7(9)
C(8)	−0.348(1)	0.0240(4)	0.353(2)	5.5(8)
C(9)	−0.141(1)	0.0906(4)	−0.031(1)	4.0(7)
C(10)	−0.030(1)	0.1222(5)	0.015(1)	5.6(8)
C(11)	−0.198(2)	0.0628(4)	0.067(1)	5.5(8)
C(12)	−0.101(2)	0.0608(5)	−0.134(1)	6.3(9)
C(13)	−0.563(2)	0.1009(4)	−0.067(1)	4.3(7)
C(14)	−0.625(2)	0.0654(7)	0.024(2)	11(1)
C(15)	−0.667(1)	0.1381(4)	−0.101(1)	4.7(7)
C(16)	−0.513(2)	0.0774(7)	−0.173(2)	11(1)
C(17)	−0.561(1)	0.2061(4)	0.264(1)	3.8(6)
C(18)	−0.592(1)	0.2385(4)	0.158(1)	3.7(6)
C(19)	−0.740(1)	0.2365(4)	0.116(1)	4.4(7)
C(20)	0.172(1)	0.2637(4)	0.198(1)	3.8(7)
C(21)	0.028(1)	0.2570(4)	0.160(1)	3.4(6)
C(22)	−0.062(1)	0.2837(4)	0.244(1)	3.3(6)

[a] $B_{eq} = {}^8/_3\pi^2(U_{11}(aa^*)^2 + U_{22}(bb^*)^2 + U_{33}(cc^*)^2 + 2U_{12}(aa^*bb^*) \times \cos\gamma + 2U_{13}(aa^*cc^*)\cos\beta + 2U_{23}(bb^*cc^*)\cos\alpha)$.

Table 6. Selected Interatomic Distances (Å) and Angles (deg) for $\{Zn[O_2P(O^tBu)_2]_2[H_2N(CH_2)_6NH_2]\}_n$ (3)

(a) Bond Distances

Zn−O(1)	1.972(7)	P(2)−O(7)	1.591(8)
Zn−O(5)	1.855(9)	P(2)−O(8)	1.566(8)
P(1)−O(1)	1.498(8)	Zn−N(1)	2.050(9)
P(1)−O(2)	1.497(8)	Zn−N(2)	2.001(8)
P(1)−O(3)	1.573(8)	O(2)···N(2)	2.83(1)
P(1)−O(4)	1.572(8)	O(6)···N(1)	2.86(1)
P(2)−O(5)	1.522(9)	O(6)···N(2)	2.94(1)
P(2)−O(6)	1.469(8)	O(2)···N(1)	2.96(1)

(b) Bond Angles

O(1)−Zn−O(5)	102.9(3)	O(1)−P(1)−O(2)	116.7(4)
O(1)−Zn−N(1)	107.4(3)	O(1)−P(1)−O(3)	109.8(4)
O(1)−Zn−N(2)	111.0(3)	O(1)−P(1)−O(4)	104.5(4)
O(5)−Zn−N(1)	116.6(4)	O(2)−P(1)−O(3)	107.8(4)
O(5)−Zn−N(2)	115.7(4)	O(2)−P(1)−O(4)	110.3(4)
N(1)−Zn−N(2)	103.1(3)	O(5)−P(2)−O(6)	117.9(5)
Zn−O(1)−P(1)	121.6(5)	O(5)−P(2)−O(7)	110.2(5)
Zn−O(5)−P(2)	162.7(6)	O(5)−P(2)−O(8)	104.1(5)
Zn−N(1)−C(17)	119.8(7)	O(6)−P(2)−O(7)	104.5(5)
Zn−N(2)−C(22)	116.7(6)	O(6)−P(2)−O(8)	111.9(5)
		O(7)−P(2)−O(8)	108.0(4)

3: A colorless platelike crystal of dimensions 0.2 × 0.2 × 0.05 mm was mounted on a glass fiber using Paratone N hydrocarbon oil. Data were collected as described for compound **1**. The data were corrected for Lorentz and polarization effects. An absorption correction was performed using XPREP (μR = 0.05, T_{max} = 0.91, T_{min} = 0.73). The 9714 integrated reflections were averaged in point group 2/*m* to give 4292 unique reflections (R_{int} = 0.090). Of these, 2407 reflections were considered observed ($I > 3.00\sigma(I)$). No decay correction was necessary. Inspection of the systematic absences uniquely

Table 7. Crystallographic Data for Compounds 1−3

	2	**1**	**3**
	(a) Crystal Parameters		
formula	$C_{48}H_{108}O_{25}P_6Zn_4$	$C_{32}H_{72}P_4O_{16}Zn_2$	$C_{22}H_{52}N_2O_8P_2Zn$
formula weight	1532.6	967.57	599.99
cryst color, habit	colorless, block	colorless, block	colorless, platelike
cryst size, mm	0.4 × 0.3 × 0.2	0.12 × 0.11 × 0.10	0.20 × 0.20 × 0.05
crystal system	monoclinic	monoclinic	monoclinic
space group	*C*2/*c*	$P2_{1/c}$	$P2_{1/c}$
a, Å	35.408(11)	20.0367(8)	10.1988 (9)
b, Å	20.232(6)	13.3832(5)	28.467 (3)
c, Å	26.447(9)	17.6697(7)	11.236 (1)
β, deg	103.60(4)	91.345(1)	93.035 (2)
volume, Å^3	18415(10)	4736.9(6)	3257.5(4)
Z	8	4	4
ρ (calc), g cm^{-3}	1.16	1.357	1.223
μ (Mo Kα), cm^{-1}	11.8	12.07	8.92
temp, °C	23	−117.0	−95.0
	(b) Data Collection		
diffractometer	Siemens P4	Siemens SMART	Siemens SMART
radiation	Mo Kα (*λ* = 0.710 69 Å)	Mo Kα (*λ* = 0.710 69 Å)	Mo Kα (*λ* = 0.710 69 Å)
scan type	2*θ*−*θ*	*ω* (0.3°/frame)	*ω* (0.3°/frame)
scan rate	4.0 to 20.0°/min in *ω*	30.0 s/frame	30.0 s/frame
rflns collected	12 357	19132	9714
unique rflns	12 037 (R_{int} = 0.056)	7205 (R_{int} = 0.086)	4292 (R_{int} = 0.090)
no. of obsns	4536 ($I > 5.0\sigma(I)$)	4053 ($I > 3.00\sigma(I)$)	2407 ($I > 3.00\sigma(I)$)
	(c) Refinement		
rfln/param ratio	8.7	8.32	7.62
R(*F*), %	8.5	7.5	8.5
R(*wF*), %	11.3	7.8	8.6
GOF	1.42	2.59	2.94
max/min peak in final diff map, e Å^{-3}	0.91/−0.61	1.15/−0.59	0.95/−0.54

defined the space group as $P2_1/c$. The structure was solved using direct methods (SAPI91), expanded using Fourier techniques (DIRDIF92), and refined by full-matrix least-squares methods using teXsan software. The non-hydrogen atoms were refined anisotropically. The hydrogen atoms were included at calculated positions but were not refined. The number of variable parameters was 316 giving a data/parameter ratio of 7.62. The maximum and minimum peaks on the final difference Fourier map corresponded to 0.95 and −0.54 e$^-$/Å^3: $R = 0.085$, $R_w = 0.086$, GOF = 2.94.

Acknowledgment. This work was supported by the Director, Office of Energy Research, Office of Basic Energy Sciences, Chemical Sciences Division, of the U.S. Department of Energy under Contract No. DE-AC03-76SF00098. We also thank Dr. Fred Hollander of the departmental X-ray facility (CHEXRAY) for determination of the crystal structure of **3**.

Supporting Information Available: Atom-labeling schemes, tables of crystal, data collection, and refinement parameters, bond distances and angles, and anisotropic displacement parameters (42 pages). This material is contained in many libraries on microfiche, immediately follows this article in the microfilm version of the journal, can be ordered from ACS, and can be downloaded from the Internet; see any current masthead page for ordering information and Internet access instructions.

CM9603821